ARTICLE
Journal of Cellular Biochemistry 113:3039–3050 (2012)

Journal of Cellular Biochemistry

Scaffold Attachment Factor B (SAFB)1 and SAFB2 Cooperatively Inhibit the Intranuclear Mobility and Function of ERα

Takashi Hashimoto, Ken-Ichi Matsuda, and Mitsuhiro Kawata*

Department of Anatomy and Neurobiology, Kyoto Prefectural University of Medicine, Kawaramachi Hirokoji, Kamigyo-ku, Kyoto 602-8566, Japan

ABSTRACT

Estrogen receptor alpha (ERα) plays a key role in physiological and pathophysiological processes as a ligand-activated transcriptional factor that is regulated by cofactors. ERα-mediated transcriptional regulation is closely correlated with the mobility of ERα in the nucleus in association with the nuclear matrix, the framework for nuclear events including transcription. However, the relationship between ERα mobility and the cofactors of ERα is unclear. Scaffold attachment factor B1 (SAFB1) and its paralog SAFB2 are nuclear matrix binding proteins that have been characterized as ERα corepressors. Here, using chimeric fluorescent proteins (FPs), we show that SAFB1 and SAFB2 colocalize with ERα in the nucleus of living cells after 17β-estradiol (E2) treatment. Co-immunoprecipitation (co-IP) experiments indicated that ERα interacts with both SAFB1 and SAFB2 in the presence of E2. Fluorescence recovery after photobleaching analysis revealed that SAFB1 and SAFB2 each decrease ERα mobility, and interestingly, coexpression of SAFB1 and SAFB2 causes a synergistic reduction in ERα dynamics under E2 treatment. In accordance with these mobility changes, ERα-mediated transcription and proliferation are cooperatively inhibited by SAFB1 and SAFB2. These results indicate that SAFB1 and SAFB2 are crucial repressors for ERα dynamics in association with the nuclear matrix and that their synergistic regulation of ERα mobility is sufficient for inhibiting ERα function. J. Cell. Biochem. 113: 3039–3050, 2012.

KEY WORDS: ERα; SAFB; NUCLEAR MATRIX; COREPRESSOR; INTRANUCLEAR MOBILITY; TRANSCRIPTION; CELL PROLIFERATION

Estrogen receptor alpha (ERα) regulates biological and physiological processes including development, reproduction, homeostasis, and maintenance in a diverse range of tissues [Kawata et al., 2001]. ERα-mediated regulation is based on the function of ERα as a ligand-activated transcription factor that controls expression of estrogen-responsive genes involved in each cellular process [McKenna et al., 1999; Moggs and Orphanides, 2001; Osborne et al., 2001; Inoue et al., 2002]. Upon ligand activation, steroid receptors form foci associated with the nuclear matrix, which is a skeletal structure related to many nuclear functions including transcription [Verheijen et al., 1988; Tsutsui et al., 2005]. A recent report showed that a progesterone receptor mutant lacking binding ability to the nuclear matrix failed to form nuclear foci, with a resulting deficit in its transcriptional activity [Graham et al., 2008], suggesting the physiological significance of cluster formation of steroid receptors.

ERα exhibits discrete cluster formation in the presence of ligand [Htun et al., 1999; Hager et al., 2000; Stenoien et al., 2000; Matsuda et al., 2002; Matsuda et al., 2008; Amita et al., 2009] and analyses using fluorescent protein (FP) as a molecular tag have provided insights into ERα dynamics in the nucleus. FP-tagged ERα (FP-ERα) is exclusively localized in the nucleus without ligand, but shows marked redistribution from a reticular to a punctate pattern upon addition of ligand. The redistributed FP-ERα is associated with the nuclear matrix [Stenoien et al., 2000] and the change in distribution is accompanied by an intranuclear mobility shift of ERα [Stenoien et al., 2001b; Ochiai et al., 2003]. Previous studies using fluorescent recovery after photobleaching (FRAP) revealed that ATP and proteasomes are required for the mobility of FP-ERα in the absence and presence of ligand [Amita et al., 2009]. In addition, cofactors that modulate ERα-mediated transcriptional activity positively and negatively [Hart and Davie, 2002; Dobrzycka et al., 2003] are

Grant sponsor: KAKENHI, Japan; Grant numbers: KAKENHI20700292, KAKENHI20240036.
*Correspondence to: Prof. Mitsuhiro Kawata, Department of Anatomy and Neurobiology, Kyoto Prefectral University of Medicine, Kawaramachi Hirokoji, Kamigyo-ku, Kyoto 602-8566, Japan. E-mail: mkawata@koto.kpu-m.ac.jp
Manuscript Received: 12 January 2012; Manuscript Accepted: 27 April 2012
Accepted manuscript online in Wiley Online Library (wileyonlinelibrary.com): 4 May 2012
DOI 10.1002/jcb.24182 • © 2012 Wiley Periodicals, Inc.

correlated with ERα mobility [Stenoien et al., 2000; Stenoien et al., 2001b; Maruvada, 2002; Wu et al., 2006]. It has been shown that the ligand-activated glucocorticoid receptor undergoes rapid and continuous exchange in an active promoter of a target gene, suggesting that the dynamic nature of steroid hormone receptors is necessary for their function as transcription factors [McNally et al., 2000]. However, while a variety of cofactors that interact with ERα have been identified, the relationship between ERα dynamics and the function of these cofactors is still unclear.

Scaffold attachment factor B1 (SAFB1) was initially discovered as a nuclear matrix binding protein. SAFB1 harbors a N terminal SAF-BOX DNA binding motif through which it interacts with a DNA element called a scaffold/matrix attachment region (S/MAR) and indirectly binds to nuclear matrix [Oesterreich, 2003; Garee and Oesterreich, 2010]. SAFB1 binds to ERα through its central major ERα interaction domain (MEID) and represses ERα-mediated transcriptional activity via an intrinsic C-terminal transcriptional repression domain [Townson et al., 2004]. This ERα corepressor function is shared by its paralog, SAFB2 [Oesterreich, 2003; Townson et al., 2003]. SAFB1 and SAFB2 are involved in cellular processes including proliferation, stress response, and apoptosis [Oesterreich, 2003; Garee and Oesterreich, 2010], but the molecular mechanism underlying the transcriptional suppression is unknown. Based on the nuclear matrix and ERα binding properties of SAFB1 and SAFB2, we hypothesized that modulation of ERα mobility by these proteins may be responsible.

In the present study, we examined the subnuclear distribution and interactions of SAFB1, SAFB2, and ERα in the absence or presence of estrogen, using FP-tagged chimeric proteins. FRAP analysis revealed a synergistic effect of SAFB1 and SAFB2 on the mobility of ligand-bound ERα in living cells. Reduction of the intranuclear mobility of ERα by SAFB1 and SAFB2 was correlated with the transcriptional activity of ERα and the resulting cellular proliferative response. These findings provide new insights into ERα-mediated transcriptional regulation through modulation of its molecular dynamics.

MATERIALS AND METHODS

PLASMID CONSTRUCTION

Expression plasmids for GFP-SAFB1 and GFP-SAFB2 were kindly provided by Prof. Steffi Oesterrich, Baylor College of Medicine [Townson et al., 2003]. To generate the pEY/CFP-SAFB1 and pEY/CFP-SAFB2 constructs, the plasmids were digested with EcoRI and the genes were then subcloned into pEG/C/YFP-C1 vectors (Clontech Laboratories, Palo Alto, CA) cut with the same restriction enzymes. A CFP-tagged SAFB1 deletion mutant (CFP-SAFB1Δ) that lacks most (aa 437-598) of the major ERα interaction domain (aa 426–600) [Townson et al., 2004] was generated from the pECFP-SAFB1 construct. After FbaI digestion, the 1187- and 1345-base pair fragments were purified with QIAquick Gel Extraction Kit (Qiagen, Chatsworth, CA) and then ligated together in ligation mix (Takara shuzo, Kyoto, Japan), followed by purification using a MinElute reaction clean up kit (Qiagen). Correct insertion was verified by XhoI restriction enzyme digestion. YFP/CFP-ERα constructs have been previously described [Matsuda et al., 2002]. To construct the RFP-ERα plasmid, the YFP-ERα vector was digested with XhoI-EcoRI and the fragments were subcloned into a pHcRed-Tandem-C1 vector (Evrogen, Moscow, Russia).

CELL CULTURE AND TRANSFECTION

Saos-2 and COS-1 cells were cultured in DMEM (Invitrogen, Carlsbad, CA) supplemented with 10% fetal bovine serum (FBS) and 1% penicillin/streptomycin (Invitrogen) in a CO_2 incubator at 37°C with 5% CO_2/95% air. Transfections were performed with LipofectAmine Plus reagent and Opti-MEM (both Invitrogen) according to the manufacturer's instructions. For ligand stimulation, cells were treated with 10^{-8} M estradiol (E2) (Sigma, St. Louis, MO) at 37°C.

CONFOCAL FLUORESCENT MICROSCOPY

For live cell imaging, the culture medium was replaced with Opti-MEM (Invitrogen) and image acquisition was performed with a LSM510 META confocal microscope (Carl Zeiss, Oberkochen, Germany) equipped with a CO_2-controlled on-stage heating chamber and argon and HeNe-1 (543 nm) lasers. YFP fluorescence was detected using a filter set at 514 nm excitation and 530–600 nm emission with a 458/514 nm dichroic mirror, and CFP fluorescence was observed using a filter set at 458 nm excitation and 475–525 nm emission with a 458/514 nm dichroic mirror. RFP, Alexa546 and CMXRos (see proliferation assay) fluorescences were viewed using a filter set at 543 nm excitation and 560–615 nm emission with a 488/543 nm dichroic mirror. All experiments were conducted at 37°C and images were analyzed using software supplied with the confocal laser microscope.

WESTERN BLOTTING (WB)

One day before the transfection experiments, 5×10^5 COS-1 cells and Saos-2 cells were plated on 35-mm culture dishes (Falcon; Becton-Dickinson Labware, Lincoln Park, NJ). COS-1 cells were transfected with pECFP/YFP-SFAB1 (3 μg), pECFP-SAFB1Δ (3 μg), pECFP/YFP-SAFB2 (3 μg), or pEYFP/RFP-ERα (0.75 μg). After 3 h, the medium was changed to DMEM (Invitrogen). The cells were maintained for 24 h and then solubilized in sodium dodecyl sulfate (SDS) sample buffer. The cell lysates were separated by 7.5% SDS–PAGE and transferred to polyvinylidene difluoride membranes (Immunobilon-P; Millipore, Bedford, MA) using a semi-dry blotting apparatus (Trans-blot-SD; Bio-Rad Laboratories, Hercules, CA). The blotted membrane was blocked with 5% albumin in TPBS [0.02% Tris-HCl (pH 8.0), 0.05% Tween 20, and 150 mM HCl] for 1 h at room temperature (RT). Immunoblotting was performed with rabbit anti-SAFB1 (A300-811A; 1:1000 dilution; Bethyl Lab., Montgomery, TX), rabbit anti-SAFB2 (A301-112A; 1:1000 dilution; Bethyl), or rabbit anti-ERα (C1355; 1:1000 dilution; Millipore, Temecula, CA) in TPBS overnight at 4°C as the primary antibody. This was followed by treatment with alkaline phosphatase-conjugated goat anti-rabbit IgG secondary antibody (1:1000 dilution; Chemicon/Millipore) for 1 h at RT. Immunoreactive bands were visualized using a BCIP/NBT solution kit (Nacalai Tesque, Kyoto, Japan).

CO-IMMUNOPRECIPITATION (CO-IP)

COS-1 cells were plated as described above, transfected with pEYFP-ERα (3 μg) for 3 h, and cultured in Opti-MEM. After 24 h, 10^{-8} M E2 was added to the medium and the cells were cultured for 24 h. Whole cell extracts were prepared from two dishes using 400 μl of low stringency lysis buffer [Townson et al., 2003] with a slight modification [20 mM Tris HCl (pH 7.6), 150 mM NaCl, 0.1% Nonidet-P40, 1% protease inhibitor cocktail (Nacalai), 100 μg/ml DNase I (Roche Diagnostics, Mannheim, Germany), 50 μg/ml RNase A(QIAGEN, Hilden, Germany)]. Cell lysates were sonicated three times for 20 s on ice, and then incubated for 1 h at 37°C. After centrifugation at 13,000*g* for 10 min at 4°C using a refrigerator centrifuge (MX-301, Tomy Seiko Co., Tokyo, Japan), supernatants (100 μl) were incubated with 2 μl of anti-SAFB1 or anti-SAFB2 antibody (Bethyl) overnight at 4°C. To prevent nonspecific interactions, protein G-Sepharose beads (GE Healthcare, Uppsala, Sweden) were preblocked with lysates containing 1 mg/ml BSA overnight and then the beads were incubated with protein overnight. After washing with 500 μl of lysis buffer four times, the pellets were resuspended in SDS sample buffer and boiled for 3 min, followed by SDS–PAGE and immunoblotting as described above.

FRAP ANALYSIS

FRAP analysis was performed based on previous protocol [Schaaf and Cidlowski, 2003] with modifications. Saos-2 and COS-1 cells were grown at 1×10^5 cells/dish on glass bottom dishes (Matsunami Glass, Kishiwada, Japan) for 24 h, transfected with pECFP/YFP-SFAB1 (1 μg), pECFP-SAFB1Δ (1 μg), pECFP/YFP-SAFB2 (1 μg), or pEYFP/RFP-ERα (0.25 μg) for 3 h, and maintained in Opti-MEM for 24 h. The cells were then treated with 10^{-8} E2 for 20 min and fluorescent images (512 × 512 pixels, zoom factor 5, scan speed 9) of a single Z section using an immersion 63× objective lens were taken at time intervals after 3.0 s photobleaching at a wavelength of 514 nm (for YFP) at 25% of its maximum power or 543 nm (for RFP) at maximum laser power for 25 iterations, and the time for the prebleach image was set to 0 s. A region of interest (ROI) in randomly selected transfected cells was defined as a circle of 25 μm in diameter. These parameters were all kept fixed in the analysis. To correct for differences in expression levels of YFP-ERα between individual cells, the fluorescence intensity values at every time point were normalized to the prebleaching level, and curves of fluorescent intensities for the bleached ROI were obtained using Zeiss LSM software. Plateau values were calculated as the average of five highest values and the half-time of fluorescence recovery ($t_{1/2}$) was determined, which is defined as the time point after photobleaching at which the fluorescence values has reached to the mean between level at bleach end time and level at plateau.

IMMUNOCYTOCHEMISTRY

COS-1 cells (1×10^5 cells/dish) were seeded on glass bottom dishes (Matsunami) and transfected with pEYFP-ERα (0.25 μg) as described above. After a 24 h pre-incubation with or without E2, the cells were fixed in 4% paraformaldehyde (PFA) for 20 min at RT and treated with 25 mM glycine in PBS, and permeabilized in 100% methanol for 3 min at −20°C, followed by blocking in PBS containing 0.3% Triton X-100 and 2% BSA for 1 h at RT. They were then incubated with the rabbit anti-SAFB1 and anti-SAFB2 antibodies (IHC-00142 and A301-112A; 1:1000 dilution; Bethyl Lab) for 2 h at RT followed by Alexa546-conjugated goat anti-rabbit IgG (Invitrogen) for 1 h at RT. In the immunocytochemical preparations, the glass slips were sealed with vectashield (Vector Lab, Burlingame, CA) and observation was performed with a Zeiss LSM 510 META confocal microscope (Carl Zeiss).

TRANSCRIPTION ASSAY

Saos-2 cells were seeded at 1×10^6 cells in 35-mm culture dishes (Falcon). The next day the cells were transfected with a pERE-luciferase reporter plasmid [Maruyama et al., 1998] (2 μg) and a β-actin promoter-driven-galactosidase expression plasmid as an internal control (2 μg). The cells were cotransfected with various combinations of YFP-ERα, CFP-SAFB1, CFP-SAFB2, and CFP-SAFB1Δ (20 ng, respectively) and cultured in Opti-MEM. After 24 h, the cells were treated with 10^{-8} E2 for a further 24 h. Controls were not treated with E2. Luciferase assays were carried out as previously described [Matsuda et al., 2002; Kitagawa et al., 2009]. Briefly, luciferase activities in cell lysates were measured by Pica Gene (Tokyo Inki, Tokyo, Japan). The luciferase activities from triplicate experiments were averaged after normalization based on the β-galactosidase activity from the same supernatants.

PROLIFERATION ASSAY

Saos-2 cells (1×10^4/cells/well) were homogenously seeded onto PLL-coated circular coverslips (Fisher Scientific, Pittsburgh, PA) in 24-well tissue culture plates (Costar, Cambridge, MA) in culture medium [Opt-MEM with 10% charcoal-stripped FBS (Invitrogen)] for 24 h. The cells were cotransfected with various combinations of pEYFP-ERα (50 ng), pECFP-SAFB1 (250 ng), pECFP-SAFB2 (250 ng), and pECFP-SAFB1Δ (250 ng) constructs. The total amount of plasmids was equalized by the addition of corresponding empty vectors, pECFP-C1 and pEYFP-C1. Cells were incubated for 3 h, followed by a medium change to culture medium with or without 10^{-8} M E2 (assay medium). WST-8 assays were performed in triplicate using a cell counting kit-8 (CCK-8) (Dojindo Laboratories, Kumamoto, Japan) at 1, 3, and 5 days after transfection. Opti-MEM medium was preincubated with 10% CCK-8 assay solution 30 min before the assay and then added to the cells (500 μl/well) after removing the assay medium. After 2 h, medium containing generated water-soluble formazan was placed in a new 24-well plate and the absorbance at 450 nm was measured immediately. At the same time, fresh assay medium was added to the culture. After performance of the WST-8 assay at 5 days post-transfection, the cells were stained by MitoTracker Red CMXRos (Molecular Probes, Eugene, OR), a dye for active mitochondria in live cells, at a final concentration of 200 nM and cultured in a 37°C incubator for 30 min. The cells were then fixed in 4% PFA for 10 min at RT, washed with PBS, and mounted onto glass slides. Confocal images (1,024 × 1,024 pixels) of a Single Z section were captured with a 20× objective lens and the number of the cells with intense red fluorescent was counted in eight random fields of view.

STATISTICAL ANALYSIS

Data are expressed as means ± SEM. The significance of differences was determined using one way analysis of variance (ANOVA) followed by a Tukey–Kramer post hoc test. $P < 0.05$ was considered statistically significant.

RESULTS

CONSTRUCTS OF FP-TAGGED SAFB1, SAFB2, AND ERα

Cyan (CFP) and yellow (YFP) fluorescent proteins were tagged to the N termini of wild type SAFB1 and SAFB2 (CFP/YFP-SAFB1, CFP/YFP-SAFB2) and a SAFB1 mutant (CFP-SAFB1Δ) in which a large part of the ERα interaction domain (aa437-598) was deleted (i.e., abrogating binding to ERα) (Fig. 1A). Expression plasmids of ERα fusion proteins with CFP, YFP [Matsuda et al., 2002], and red fluorescent protein (RFP) were also prepared. Using antibodies specific to SAFB1, SAFB2, or ERα, WB analysis of transiently transfected COS-1 and Saos-2 cells was performed to confirmed expression of proteins of appropriate sizes (Fig. 1B).

DISTRIBUTION OF SAFB1, SAFB2, AND ERα IN THE NUCLEUS

To examine the subnuclear distribution patterns of SAFB1 and SAFB2 under estrogen-stimulated and estrogen-free conditions, transient cotransfection with YFP-SAFB1 or YFP-SAFB2 and CFP-ERα expression vectors was performed in Saos-2 cells that were then subjected to live cell imaging with or without E2 treatment. Saos-2 cells do not express endogenous SAFB1 and SAFB2 (Fig. 1B) because of a homozygous deletion at the D192216 locus [Townson et al., 2003; Townson et al., 2004]. Confocal laser microscopy revealed punctate patterns of YFP-SAFB1 and YFP-SAFB2 distribution in the nucleus in the presence or absence of E2 (Fig. 2A–F, middle panels). The intranuclear distribution of CFP-ERα showed a ligand-dependent change from a diffusely homogenous pattern to a discrete dot pattern (Fig. 2A–F, left panels) as reported previously [Htun et al., 1999; Hager et al., 2000; Stenoien et al., 2000; Kawata et al., 2001; Matsuda et al., 2002; Matsuda et al., 2008; Amita et al., 2009]. Colocalization of fluorescent signals of CFP-ERα clusters with exogenous YFP-SAFB1 and YFP-SAFB2 were also detected (Fig. 2D,F). We performed additional immunocytochemical studies to examine subnuclear localization of ERα, endogenous SAFB1, and SAFB2 (Fig. 1G–L). COS-1 cells were transfected with YFP-ERα alone, maintained in medium containing or lacking E2, fixed, and then stained for SAFB1 or SAFB2. Addition of E2 changed the diffuse nucleoplasmic pattern of YFP-ERα (Fig. 2G,I,K, left panels) to a punctate pattern (Fig. 2H,J,L, left panels), and again we observed colocalization of YFP-ERα signal with SAFB1 and SAFB2 immunoreactivity (Fig. 2J,L) in response to E2 exposure. These observations indicate that subnuclear localization of SAFB1 and SAFB2 is confined to particular regions, possibly on the nuclear matrix, and that ligand-activated ERα accumulates at the same sites in the nucleus.

SAFB1 AND SAFB2 INTERACT WITH ERα IN THE PRESENCE OF E2

Based on the colocalization of ERα with the two SAFB proteins described above, we postulated that the interactions of SAFB1 and SAFB2 with ERα may be strengthened in a ligand-dependent

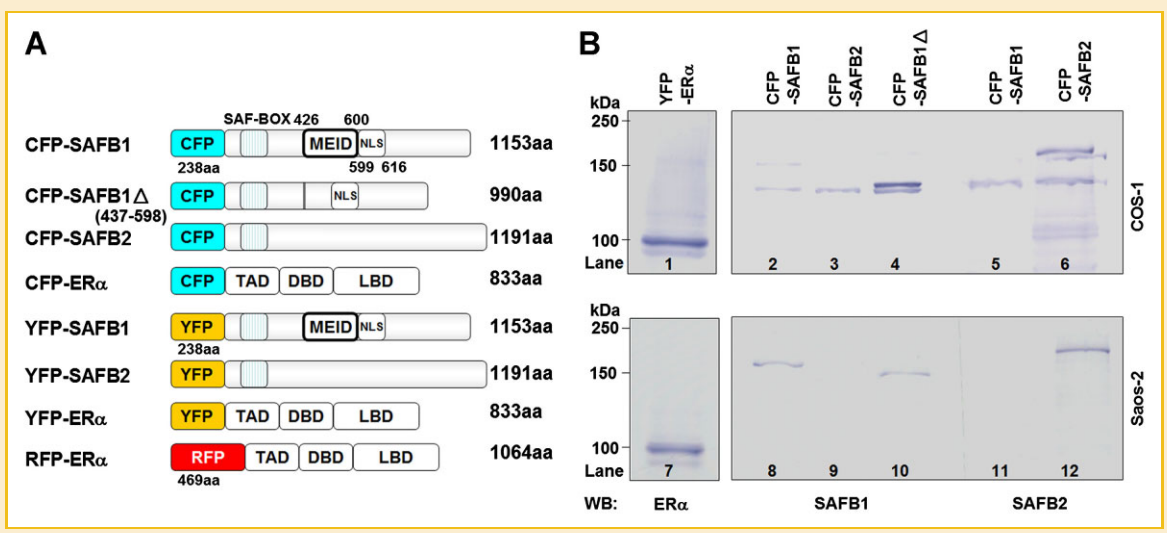

Fig. 1. Constructs of SAFB1, SAFB1 deletion mutant, SAFB2 and ERα tagged with FP-color variants. A: Plasmid construction of CFP (cyan fluorescent protein)- and YFP (yellow fluorescent protein)-tagged full length SAFB1 and SAFB2, CFP-tagged SAFB1 deletion mutant, and CFP/YFP/RFP-fused ERα proteins. SAF-BOX, scaffold attachment factor box; MEID, major ERα interaction domain; NLS, nuclear localization signal; TAD, transactivation domain; DBD, DNA-binding domain; LBD, ligand binding domain. B: Immunoblotting analysis of fusion proteins. YFP-ERα was detected as an immunoreactive band of 95 kDa (lane 1, 7). Endogenous SAFB1 and transiently expressed CFP-SAFB1 proteins in COS-1 cells migrated at approximately 130 kDa (lanes 2–4) and 157 kDa (lane 2), respectively. The CFP-SAFB1 deletion mutant formed a band at a predicted molecular mass of 139 kDa (lane 4). Compared to the bands for SAFB1 and CFP-SAFB1 (lane 2), polyclonal anti-SAFB2 antibody detected slightly higher molecular weight bands from SDS extracts of COS-1 cells transfected with pECFP-SAFB2 (lane 6). Bands representing CFP-ERα and YFP-SAFB1 were also detected at the expected molecular sizes of 95 and 157 kDa, respectively (data not shown). Expression of RFP-ERα and YFP-SAFB2 was also verified (Fig. 5A). In contrast, no specific bands for endogenous SAFB1 and SAFB2 were detected from lysates of SAFB1- and SAFB2-negative Saos-2 cells (lanes 8–12). The bands in lanes 2–6 or 8–12 were detected on the same blot, respectively.

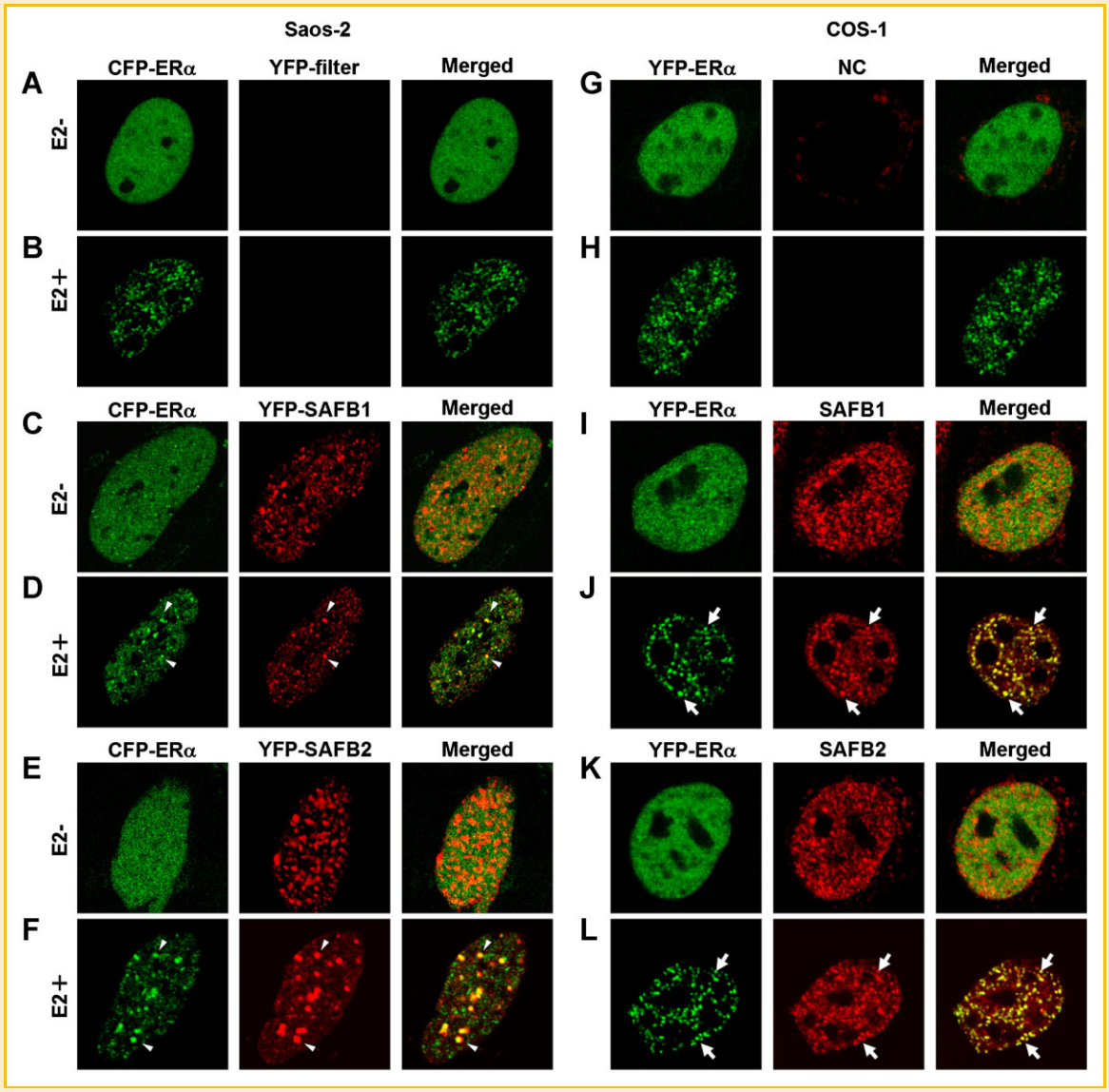

Fig. 2. Colocalization of ERα with SAFB1 and SAFB2 in the nucleus. A–F: Saos-2 cells were transfected with CFP-ERα (pseudo-colored green), YFP-SAFB1, and YFP-SAFB2 (pseudo-colored red). Confocal live cell images showed a diffuse distribution of ERα (A, C and E, left panel) and a punctate pattern of YFP-SAFB1 and YFP-SAFB2 in the nucleus under E2-free condition (A, C, and E, middle panel). Treatment of cells with 10^{-8} M E2 for 20 min produced punctate colocalization of CFP-ERα with YFP-SAFB1 and YFP-SAFB2 (D, F, arrowheads). G–L: COS-1 cells transfected with YFP-ERα (pseudo-colored green) were fixed, permeabilized, and stained with anti-SAFB1 and SAFB2 antibodies (pseudo-colored red). E2 treatment changed the intranuclear distribution of YFP-ERα into a punctate pattern and the dots were colocalized with SAFB1 and SAFB2 immunoreactive puncta (J, L, arrows). NC: Negative control (without primary antibody). Bars, 10 μm.

manner. To investigate these interactions, the YFP-ERα expression vector was introduced into COS-1 cells that endogenously express both SAFB1 and SAFB2. After incubating the cells with or without E2, co-IP assays were carried out with SAFB1 and SAFB2 antibodies (Fig. 3A–F). Although no ERα-immunoreactive bands were found in immunoprecipitates from cells cultured without E2 (Fig. 3C), YFP-ERα was expectedly detected in anti-SAFB1 and anti-SAFB2 immunoprecipitates of E2-treated cells as single bands of 95 kDa (Fig. 3F). The same immunoprecipitated samples were tested by WB analysis with anti-SAFB1 and anti-SAFB2 antibodies, and interestingly the lysates contained both SAFB1 and SAFB2 in the absence or presence of E2 (Fig. 3A,B and D,E, respectively). These findings show that ERα interacts with SAFB1 and SAFB2 in response to ligand binding and suggest that SAFB1 and SAFB2 form oligomeric complexes.

SAFB1 AND SAFB2 DECREASE THE INTRANUCLEAR MOBILITY OF LIGAND-BOUND ERα

On the basis of the above results, we hypothesized that ligand-mediated redistribution of ERα is accompanied by colocalization and interactions with SAFB1 and SAFB2, which make ERα less mobile. Photobleaching analysis was used to evaluate the effect of SAFB1 and SAFB2 expression on the intranuclear mobility of ERα in the presence of ligand. COS-1 and Saos-2 cells were singly or

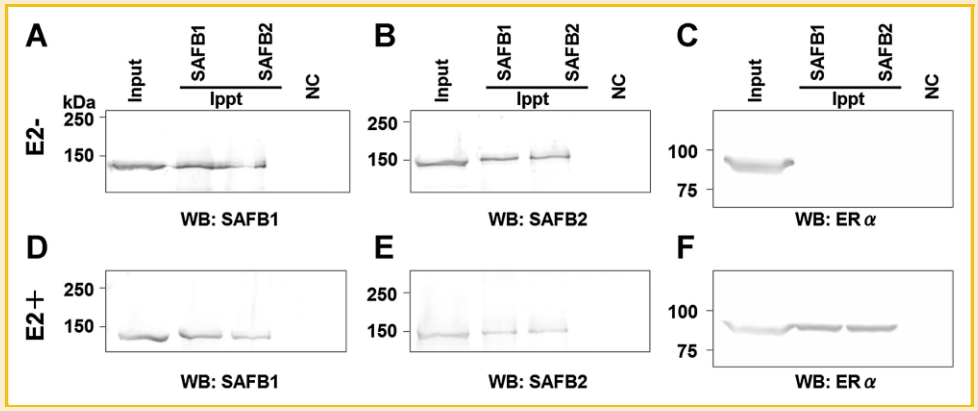

Fig. 3. Interactions of SAFB1 and SAFB2 with ERα in the nucleus under E2 treatment. A–C: COS-1 cells were transfected with pEYFP-ERα and cultured without E2. Nuclease-treated cell lysates were subjected to immunoprecipitation (IP) with antibodies against SAFB1 and SAFB2. Input (40%) and immunoprecipitated samples were immunoblotted with anti-SAFB1 (A), anti-SAFB2 (B), and anti-ERα (C) antibodies. Lysates immunoprecipitated with G-Sepharose alone were loaded as a negative control (NC). No bands corresponding to ERα were detected in the immunoprecipitated samples with antibodies against SAFB1 and SAFB2 (C), whereas bands for SAFB1 (A) and SAFB2 (B) were detected. D–F: COS-1 cells were transfected with pEYFP-ERα and cultured in the presence of 10^{-8} M E2 for 24 h. Note the robust immunoreactive band representing exogenous ERα (F).

multiply transfected with various combinations of plasmids encoding YFP-ERα, CFP-SAFB1, CFP-SAFB1Δ, and CFP-SAFB2 (Fig. 4I), and then maintained in serum-free medium for 24 h. The cells were then treated with E2 for 20 min and a randomly selected region was bleached, with the pre-bleach image defined as time 0. In the experiments using Saos-2 cells except that with cotransfection of YFP-ERα, CFP-SAFB1, and CFP-SAFB2 (Fig. 4C,D,F,G), no apparent delay in fluorescence recovery was observed compared to

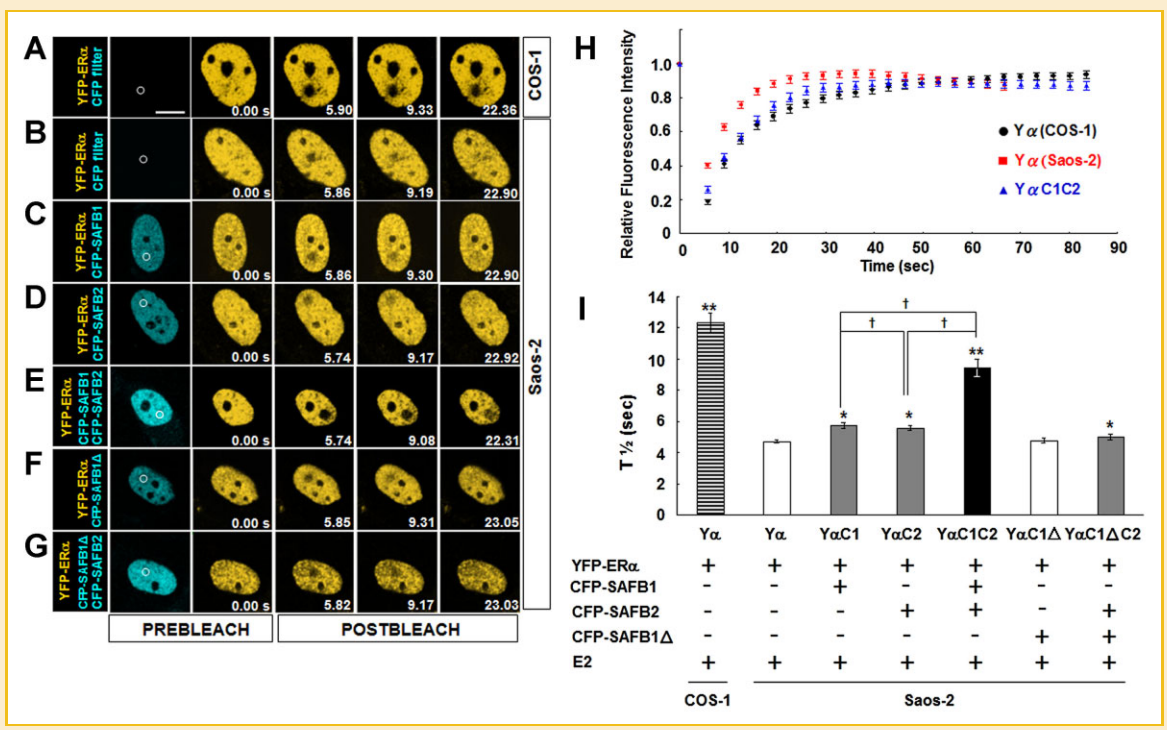

Fig. 4. Influence of coexpression of SAFB1 and SAFB2 on the intranuclear mobility of YFP-ERα in the presence of E2. A–G: Analysis of fluorescence recovery of YFP-ERα. Saos-2 cells were cotransfected with the indicated combinations of plasmids expressing YFP-ERα, CFP-SAFB1, CFP-SAFB2, and CFP-SAFB1Δ followed by E2 treatment and FRAP analysis in a circle of 2.5 μm radius. Representative images (pre-bleach, t = 0.0 s) in the FRAP analysis are shown. The areas of bleach spots are indicated by white circles. Triply transfected Saos-2 cells with the YFP-ERα/CFP-SAFB1/CFP-SAFB2 vector construct (E) showed higher CFP fluorescent intensity and the bleach spot remained dark for a longer time compared to cells in other transfection experiments (B–D, F, and G) as well as transfected COS-1 cells with YFP-ERα (A). Bars. 10 μm. H: Representative recovery curves from FRAP analysis of YFP-ERα in COS-1 cells (circles), Saos-2 cells (squares), and transfected Saos-2 cells with CFP-SAFB1 and CFP-SAFB2 vectors (triangles). Fluorescence insensitivity at each time point was normalized to that at 0 s of 1.0, averaged (n = 20 cells), and plotted. I: Half-time fluorescence recovery ($t_{1/2}$) are expressed as a mean ± SEM from a total of 60 cells (20 cells from three independent experiments). $^{*}P < 0.005$ versus Yα; $^{**}P < 0.0005$ versus Yα; $^{\dagger}P < 0.05$ (one-way ANOVA).

single transfection with YFP-ERα (Fig. 4B) and fluorescence recovery was almost complete within 23.0 s. In cotransfection with YFP-ERα, CFP-SAFB1, and CFP-SAFB2 expressing plasmids, some cells exhibited brighter CFP fluorescence in the nucleus compared with surrounding CFP-positive cells (Fig. 4E), indicating coexpression of CFP-SAFB1 and CFP-SAFB2. FRAP analysis in the high CFP cells revealed a clear dark spot in the nucleus at approximately 6.0 s that took more than 23.0 s for full recovery of fluorescence, and this recovery time course was similar to that observed in YFP-ERα transfected COS-1 cells (Fig. 4A), suggesting that the mobility of YFP-ERα was reduced by coexpression of SAFB1 and SAFB2. Normalized fluorescence recovery curves clearly indicated that the mobility of YFP-ERα in Saos-2 cells transfected with both SAFB genes was less dynamic than that in wild type Saos-2 cells, and was parallel to that observed in COS-1 cells (Fig. 4H). However, this delay of fluorescence recovery was not detected in cells cotransfected with YFP-ERα, CFP-SAFB1Δ, and CFP-SAFB2 (Fig. 4G).

To quantify the mobility of ERα, the half-time of fluorescence recovery ($t_{1/2}$) of liganded YFP-ERα was measured (Fig. 4I). Consistent with the changes in affinity shown in Figure 3C,F, coexpression of YFP-ERα with CFP-SAFB1 or CFP-SAFB2 resulted in significant decreases in the mobility of liganded YFP-ERα compared to YFP-ERα alone ($t_{1/2}$, 5.74 ± 0.21 s or 5.56 ± 0.15 s vs. 4.71 ± 1.13 s; $n = 20$). In contrast, when the cells were transfected with the CFP-SFAB1Δ plasmid, fluorescence of liganded YFP-ERα recovered on a time scale that did not differ significantly from that with YFP-ERα alone ($t_{1/2}$, 4.77 ± 0.15 s; $n = 20$). Intriguingly, quantitative FRAP analysis showed a marked decrease in YFP-ERα dynamics in triple transfection experiments in Saos-2 cells with YFP-ERα, CFP-SAFB1, and CFP-SAFB2 ($t_{1/2}$, 9.41 ± 0.56 s; $n = 20$) to a statistically similar extent observed in COS-1 cells ($t_{1/2}$, 12.30 ± 0.63 s; $n = 20$). This synergistic effect was eliminated when cells were cotransfected with YFP-ERα, CFP-SAFB1Δ, and CFP-SAFB2 ($t_{1/2}$, 5.00 ± 0.18 s; $n = 20$). These results show that SAFB1 and SAFB2 individually inhibit the intranuclear mobility of ERα and that coexpression of both paralogs synergistically represses ERα mobility.

To confirm these findings, quantitative FRAP analysis was performed using three GFP spectral variants (CFP, YFP, and RFP) that enabled the analysis to be carried out in cells in which expression of the three different proteins could be monitored. The characteristics of YFP-SAFB2 and RFP-ERα determined by WB analysis and representative images of Saos-2 cells expressing CFP-SAFB1, YFP-SAFB2, and RFP-ERα are shown in Figure 5A,B, respectively. After transfection with various combinations of constructs, FRAP analysis was used to calculate $t_{1/2}$ of liganded RFP-ERα and results similar to those described above were obtained (Fig. 5C).

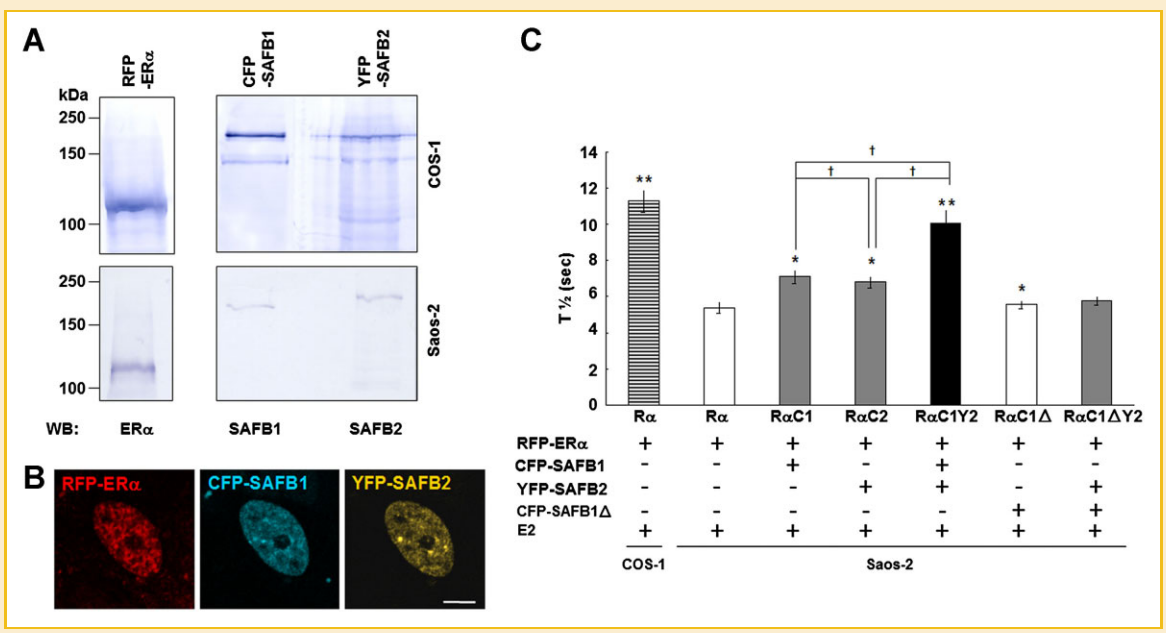

Fig. 5. Coexpression of CFP-SAFB1 and YFP-SAFB2 synergistically decreased the intranuclear mobility of RFP-ERα in the presence of E2. A: Immunoblot analysis of RFP-ERα, CFP-SAFB1, and YFP-SAFB2 from transiently transfected COS-1 and Saos-2 cells. An immunoreactive band for RFP-ERα was detected at about 120 kDa. B: Representative images of triply transfected Saos-2 cells with RFP-ERα, CFP-SAFB1, and YFP-SAFB2 vectors. Bar, 10 μm. C: Quantitative analysis of fluorescence recovery of nuclear RFP-ERα in Saos-2 cells transfected with RFP-ERα, CFP-SAFB1 or CFP-SAFB1Δ, and YFP-SAFB2 (Rα, C1, C1Δ, and Y2, respectively). Double transfection of Rα and C1 or Rα and Y2 led to a significant reduction in the mobility of liganded RFP-ERα compared to single transfection of Rα ($t_{1/2}$, 7.10 ± 0.38 s or 6.80 ± 0.31 s vs. 5.40 ± 0.30 s; $n = 10$). Double transfection of Rα and C1Δ had no effect on RFP-ERα dynamics ($t_{1/2}$, 5.56 ± 0.21 s; $n = 10$). Triple transfection of Saos-2 cells with Rα, C1 and Y2 synergistically inhibit RFP-ERα dynamics ($t_{1/2}$, 10.04 ± 0.77 s; $n = 10$) to the levels similar to that observed in COS-1 cells ($t_{1/2}$, 11.28 ± 0.62 s; $n = 10$). In contrast, such inhibitory action was not seen in the case of Saos-2 cells transfected with Rα, C1Δ and Y2 ($t_{1/2}$, 5.76 ± 0.24 s; $n = 10$). Data shown are the mean ± SEM from a total of 30 cells (10 cells from three independent experiments). $^{*}P < 0.005$ versus Rα; $^{**}P < 0.0005$ versus Rα; $^{\dagger}P < 0.006$ (one-way ANOVA).

SAFB1 AND SAFB2 REPRESS ERα-MEDIATED TRANSACTIVATION IN AN ADDITIVE MANNER

The findings from FRAP analysis that the mobility of liganded ERα was significantly affected by cooperative interactions of SAFB1 and SAFB2 raised the question of whether this mobility shift has relevance to subsequent ERα-mediated transcriptional events. Therefore, we next used a luciferase assay to assess the function of SAFB1 and SAFB2 as corepressors of ERα. E2-induced transcriptional activity for ERα was significantly suppressed in Saos-2 cells transfected with a CFP-SAFB1 or CFP-SAFB2 plasmid, and cotransfection of both plasmids resulted in additive repression of this activity (Fig. 6). Expression of CFP-SAFB1Δ failed to attenuate the enhanced transcriptional activation by E2, confirming the role of the MEID region of SAFB1 (Fig. 1A) in repression of ERα-mediated transcription and the functional properties of the fusion proteins generated in this study.

SAFB1 AND SAFB2 COOPERATIVELY INHIBIT ERα-MEDIATED CELL PROLIFERATION

Next, cell proliferation assays were conducted to examine whether SAFB1 and SAFB2 act in concert to repress ERα function at the cellular level. Saos-2 cells transfected with plasmids (as indicated in Fig. 7A) were continuously cultured in E2-free or E2-containing medium and proliferation was quantified by WST-8 assay (Fig. 7A) and evaluated by cell counting using confocal laser microscopy (Fig. 7B,C). In the WST-8 assays, there were no significant differences in proliferation rates among the groups on day 1 after transfection, but cells expressing YFP-ERα with E2 treatment (positive control) exhibited a significant increase in proliferation compared to non-treated cells (control) on day 5. In contrast, transient coexpression of YFP-ERα and CFP-SAFB1 or YFP-ERα and CFP-SAFB2 inhibited E2-stimulated proliferation (69.0 and 68.4%, respectively, relative to the positive control) and simultaneous expression of YFP-ERα, CFP-SAFB1, and CFP-SAFB2 resulted in further reduction of the proliferation rate (50.1% relative to the positive control) to a level that did not differ significantly from that of the control (Fig. 7A). Similar results were obtained from direct live cell counts (Fig. 7C). In each assay, truncation of most of the MEID of SAFB1 fully rescued E2-enhanced proliferation to a level that did not differ significantly from that of the positive control (Fig. 7A,C). These results suggest that SAFB1 and SAFB2 inhibit the cell proliferation in a cooperative manner.

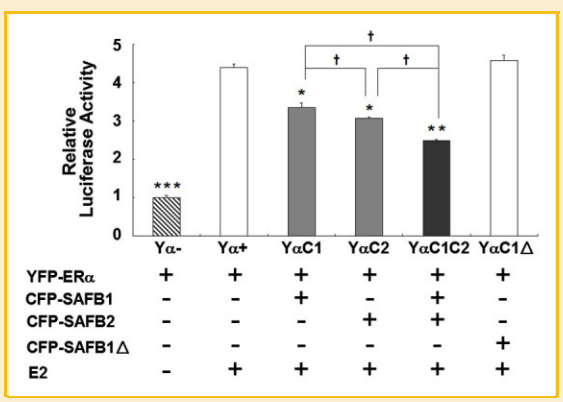

Fig. 6. Effect of SAFB1 and SAFB2 on ERα-mediated transcription. Plasmids containing estrogen-responsive element reporter (ERE-Luc) and control pAct-β-Gal genes were introduced into Saos-2 cells together with the indicated combinations of plasmids expressing YFP-ERα, CFP-SAFB1, CFP-SAFB1Δ, and CFP-SAFB2. Cell lysates were analyzed by luciferase assay with data normalized with β-Gal activity. The results are expressed relative to the activity of the pEYFP-ERα construct without E2 treatment (Yα-; set to 1.0) as the mean ± SEM from three independent experiments determined in duplicate (n = 6 for each group). $^{*}P < 0.005$ versus Yα; $^{**}P < 0.0005$ versus Yα; $^{***}P < 0.00005$ versus Yα; $^{\dagger}P < 0.05$ (one-way ANOVA).

DISCUSSION

There is accumulating evidence that nuclear events are implicated in dynamic cellular processes. Transcriptional regulation by steroid receptors is a dynamic process that is mediated by multiple mechanisms in the nucleus [McNally et al., 2000; Stenoien et al., 2001b; Hager, 2004; Rayasam et al., 2005; Hager et al., 2009]. As well as the mobility of the steroid receptor itself, interactions between steroid receptors and the nuclear matrix, the skeletal structure orchestrating the organization of DNA and placement of the nuclear machinery, are fundamental for the proper control of gene expression [Buttyan et al., 1983; DeFranco and Guerrero, 2000; McNally et al., 2000; Stenoien et al., 2001a; Schaaf and Cidlowski, 2003]. Here, we focused on unique features of SAFB1 and its paralog SAFB2, which are nuclear matrix binding proteins and ERα corepressors, and found that these proteins are the key factor that connects ERα mobility and nuclear dynamics.

We first identified the intranuclear distribution and interaction between SAFB1/SAFB2 and ERα in the presence or absence of ligand. In the nucleus of Saos-2 cells (SAFB1- and SAFB2-negative), we observed a dot distribution pattern of exogenously expressed SAFB1 and SAFB2, which was similar to the subnuclear pattern of endogenous SAFB1 and SAFB2 found in HEK293 cells [Sergeant et al., 2007]. These subnuclear patterns were unchanged by addition of E2, suggesting no direct effect of E2 on the function of SAFB1 and SAFB2. Consistent with other observations [Htun et al., 1999; Hager et al., 2000; Stenoien et al., 2000; Kawata et al., 2001; Matsuda et al., 2002; Matsuda et al., 2008; Amita et al., 2009], an E2-induced punctate distribution of FP-tagged ERα was found in Saos-2 cells, with colocalization with SAFB1 and SAFB2. Furthermore, immunocytocemistry demonstrated this colocalization of ERα with endogenous SAFB1 and SAFB2 in COS-1 cells, confirming functional properties of FP-tagged SAFB proteins. Steroid receptors including ERα are associated with the nuclear matrix [Barrack, 1987; DeFranco and Guerrero, 2000] and this matrix provides a framework for various nuclear events such as transcription, RNA processing, and hormone action [Barrack, 1987; Verheijen et al., 1988; Tsutsui et al., 2005; Graham et al., 2008]. These findings and our localization analyses support the idea that ERα could be indirectly bound to the nuclear matrix through interactions with SAFB1 and SAFB2 in the presence of ligand. Our co-IP data provide evidence that E2 induces a direct ERα interaction with endogenous SAFB1 and SAFB2. We observed this interaction in samples with nuclease treatment, suggesting that ERα was pulled down via

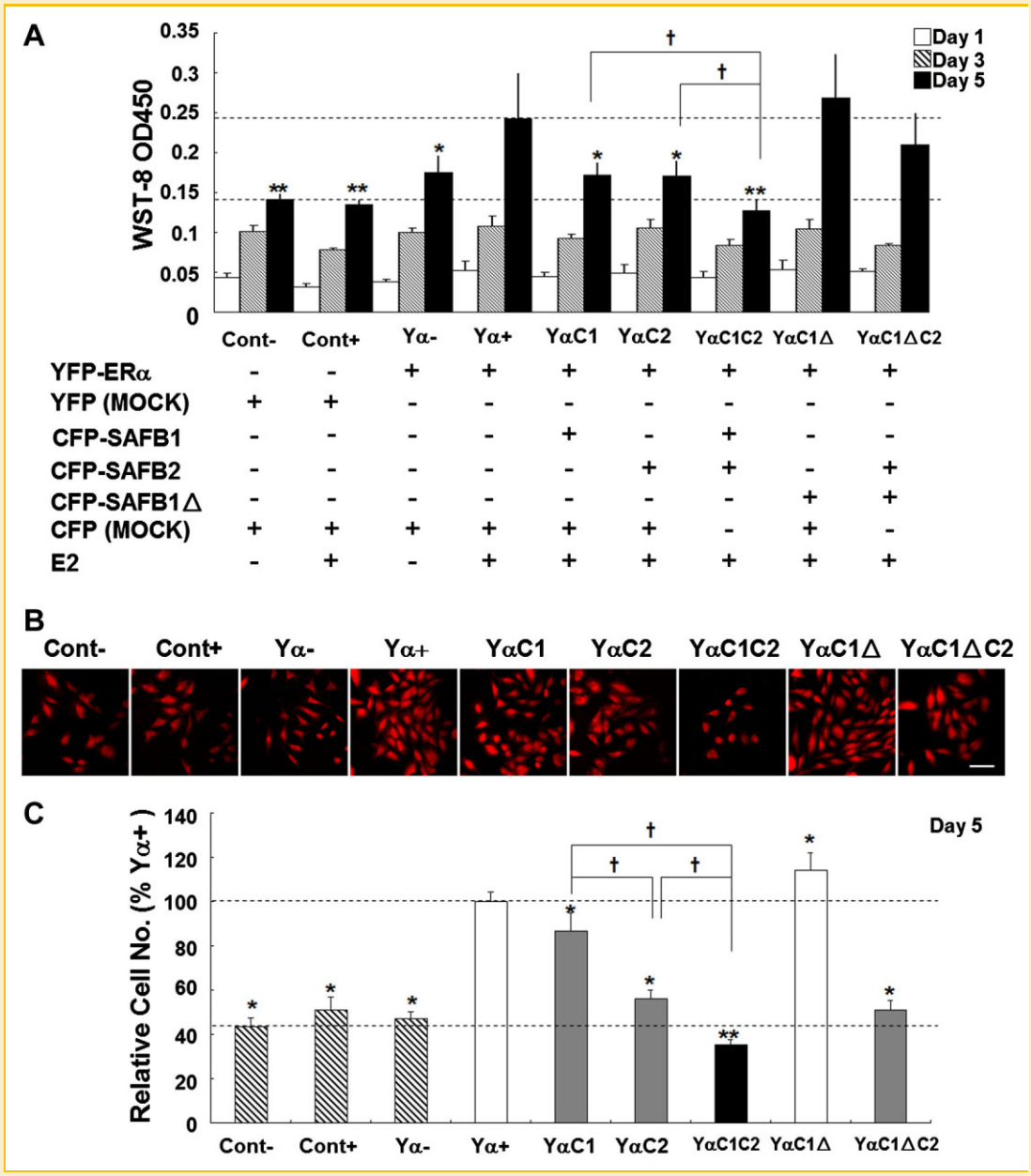

Fig. 7. Effect of cotransfection of SAFB1 and SAFB2 on ERα-mediated cell proliferation. A: Saos-2 cells were homogeneously plated on PLL-coated glass coverslips, cotransfected with the indicated combinations of plasmids expressing pECFP-C1, pEYFP-C1, CFP-SAFB1, CFP-SAFB1Δ, CFP-SAFB2 and YFP-ERα, and cultured in the presence or absence of E2. Cell proliferation was measured by WST-8 assay on days 1, 3, and 5 after transfection. Pooled data from two independent experiments each performed in triplet ($n = 6$ for each group) are shown as the mean ± SEM. $^{*}P < 0.05$ versus Yα+ on day 5; $^{**}P < 0.005$ vsersu Yα+ on day 5; **, $^{\dagger}P < 0.05$ versus Yα/C1/C2 on day 5 (one-way ANOVA). B: After the WST-assay, Saos-2 cells were stained with Mitotracker Red, a fluorescent dye for mitochondria in living cells, and fixed with 4% PFA. Typical images of the cells taken with a 20× objective lens on day 5 are shown. Bar, 100 μm. C: The average number of cells stained with Mitotracker Red was counted under a confocal microscope using a 20× objective lens (eight random fields for each dish). Pooled data from two independent experiments each performed in triplicate ($n = 48$ for each group) are shown as the mean ± SEM. The mean value of Yα+ was set to 100%. $^{*}P < 0.005$ versus Yα+ on day 5; $^{**}P < 0.0005$ versus Yα+ on day 5; **, $^{\dagger}P < 0.005$ versus Yα/C1/C2 on day 5 (one-way ANOVA).

protein–protein interaction and but not via an indirect interaction mediated by DNA. IP analyses also suggested possible hetero-oligomerization of SAFB1 and SAFB2 in the absence of E2. Previous studies have also shown an interaction between SAFB1 and SAFB2 in MCF-7 cells using a doxycycline-inducible system and untransfected HEK293 cells [Townson et al., 2003; Sergeant et al., 2007]. In addition, we detected self-association between SAFB1 and SAFB2 in the presence of E2, implying that the intimate structural and functional relationship between these proteins is preserved in the ligand-activated state.

We also evaluated the effect of SAFB1 and SAFB2 on ERα mobility in the presence of ligand and discovered that both SAFB1

and SAFB2 negatively regulate ERα dynamics. Tissues with high expression of SAFB1 also show high expression of SAFB2, and vice versa [Townson et al., 2003], and expression of both genes is thought to be regulated through one small (500 bp) bidirectional promoter [Oesterreich, 2003; Townson et al., 2003], thus facilitating interactions with each other in the nucleus. It has also been suggested that the mobility of ERα depends on its association with the nuclear matrix [Stenoien et al., 2001a]. Hence, it is highly probable that SAFB1 and SAFB2 could be causative factors in mobility loss of ligand-bound ERα in the nucleus. Consistent with other reports [Stenoien et al., 2001b; Ochiai et al., 2003; Matsuda et al., 2008], exogenous ERα was extremely mobile in Saos-2 cells as well as in other cell lines under E2-free condition, and we could not determined its mobility whether SAFB1 and SAFB2 are exogenously expressed or not. E2 led to notable reduction in ERα mobility with no expression of SAFB1 or SAFB2, implying there exist other elements that take part in this mobility loss and/or both paralogs have no influence on the ligand-induced translocation of ERα per se. However, quantitative FRAP analysis revealed that exogenously expressed SAFB1 in Saos-2 cells indeed caused reduction in ERα mobility under E2 condition. Besides, the same result was obtained with SAFB2 expressing plasmid, suggesting that both SAFB1 and SAFB2 have inherent inhibitory effect on ERα mobility and thereby exhibit individual functions as corepressor. Furthermore, of note, simultaneous expression of SAFB1 and SAFB2 resulted in a marked reduction of ERα dynamics to the similar level observed in transfected COS-1 cell, emphasizing significant contribution of both SAFB proteins to ERα dynamics. On the other hand, overexpression of SFAB1 or SAFB2 in COS-1 cells showed no effect on ERα mobility (data not shown), probably because there express enough endogenous both SAFB proteins.

The mobility of steroid receptors is thought to be correlated with their transcriptional activity [van Steensel et al., 1995; Kino et al., 2006; Graham et al., 2008]. Our transcriptional assays exclude the possibility that this phenomenon can be attributed to functional or structural impairment due to tagging of SAFB1 and SAFB2 with CFP, because exogenous expression of CFP-SAFB1 and CFP-SAFB2 suppressed ERα-mediated transactivation, as previously described [Townson et al., 2003]. This finding provides an explanation of the significance of coexpression of SAFB1 and SAFB2 in the nucleus. Steroid receptor-mediated transcriptional events occur on a time scale of minutes to hours [Belmont, 2003; Hager, 2004; Hager et al., 2006] and the physical dynamics of the nuclear environment must match this relatively short period. Simultaneous expression of SAFB1 and SAFB2 may contribute to this rapid change. Concomitant association of SAFB1 and SAFB2 with an ERα dimer (i.e., a ternary complex of SAFB1, SAFB2, and ERα dimer) is predicted to facilitate the affinity of ERα for the nuclear matrix. The co-IP results in this study imply that this complex is formed in a hormone-stimulated state, but the ERα binding motif in SAFB1 and SAFB2 [Townson et al., 2004], the manner in which this motif interacts with the ERα dimer, and whether SAFB1 really binds to the ERα dimer together with SAFB2 remain unknown.

The new findings from FRAP analysis shed light on the significance of the interplay between SAFB1 and SAFB2 on regulation of transcription factors. Further studies are required to elucidate the mechanisms of cooperative regulation of ERα mobility by SAFB1 and SAFB2. SAFB1 binds to other transcriptional factors such as an PPAR, p53 and RORα1 [Debril et al., 2005; Garee and Oesterreich, 2010], as well as ERα, and may influence the transcriptional activities of these factors by modulating their intranuclear mobility. This implication could represent an intriguing model for understanding the relationship between transcriptional regulation and the nuclear architecture.

In this study, we also examined the effect of SAFB1 and SAFB2 on cellular function. Consistent with previous results, Saos-2 cells overexpressing ERα show increased proliferation in response to E2 [Zhao et al., 2009]. Our results further showed that expression of SAFB1 and SAFB2 reduced cell proliferation in a cooperative manner that was correlated with transcriptional regulation. Thus, we found interplay of SAFB1 and SAFB2 at the cellular level. Overexpression of SAFB1 also inhibits proliferation of MCF-7 cells, an ERα-positive breast cancer cell line, and reduces the number of cells in S phase in ERα-negative HEK293 cells, which suggests effects of ERα-dependent and ERα-independent pathways on suppression of cell proliferation [Townson et al., 2000; Oesterreich, 2003; Townson et al., 2003; Garee and Oesterreich, 2010]. Comparison of the proliferation rates of cells expressing SAFB1 and the SAFB1 deletion mutant suggests that an ERα-dependent pathway is mainly involved in this process at least in Saos-2 cells. Therefore, there may be cell type-specific aspects to inhibition of proliferation by SAFB1.

The current study supports the idea that the mobility of ERα depends on binding to the nuclear matrix, and that SAFB1 and SAFB2 influence the mobility of ERα. Through their interaction with ERα, SAFB1, and SAFB2 repress the intranuclear mobility, transactivation, and cell proliferative functions of ERα in a cooperative manner. Several lines of evidence support the idea that SAFB1 and SAFB2 are putative tumor suppressors. It has been reported that loss of chromosomal locus on 19p13 which SAFB1 and SAFB2 share is frequently observed in human breast cancer [Oesterreich et al., 2001; Miller et al., 2003; Hammerich-Hille et al., 2009]. Moreover, mutations in SAFB1 have been detected in breast cancer cell lines and breast tumor tissues [Oesterreich et al., 2001]. Our findings yield new insights into the modulation of ERα function via controlling its dynamics by nuclear matrix-binding proteins and may provide further understanding of the physiological significance of SAFB1 and SAFB2 including tumorigenesis suppression.

ACKNOWLEDGMENTS

We greatly appreciate the kind gift of the GFP-SAFB1 and GFP-SAFB2 plasmid constructs from Prof. Steffi Oestrreich (Baylor College of Medicine). We also thank Prof. M. Nishi and Dr. Matsunaga (Department of Anatomy and Cell Biology, Nara Medical University) for technical advice on FRAP analysis, Dr. Y. Sowa (Department of Molecular Targeting & Cancer Prevention, Kyoto Prefectural University of Medicine) for advice on Saos-2 cell culture and luciferase measurements, and Dr. Jin Da-cheng (Department of Anatomy, China Medical University) for help with vector construction.

REFERENCES

Amita M, Takahashi T, Tsutsumi S, Ohta T, Takata K, Henmi N, Hara S, Igarashi H, Takahashi K, Kurachi H. 2009. Molecular mechanism of the inhibition of estradiol-induced endometrial Epithelial cell proliferation by clomiphene citrate. Endocrinology 151:394–405.

Barrack ER. 1987. Steroid hormone receptor localization in the nuclear matrix: Interaction with acceptor sites. J Steroid Biochem 27:115–121.

Belmont A. 2003. Dynamics of chromatin, proteins, and bodies within the cell nucleus. Curr Opin Cell Biol 15:304–310.

Buttyan R, Olsson CA, Sheard B, Kallos J. 1983. Steroid receptor-nuclear matrix interactions. J Biol Chem 258:14366–14370.

Debril MB, Dubuquoy L, Fige JN, Wahli W, Desvergne B, Auwerx J, Geiman L. 2005. Scaffold attachment factor B1 directly interacts with nuclear receptors in living cells and represses transcriptional activity. J Mol Endocrinol 35: 503–517.

DeFranco DB, Guerrero J. 2000. Nuclear matrix targeting of steroid receptors: Specific signal sequences and acceptor proteins. Crit Rev Eukaryot Gene Expr 10:39–44.

Dobrzycka KM, Townson SM, Jiang S, Oesterreich S. 2003. Estrogen receptor corepressors - a role in human breast cancer? Endocr Relat Cancer 10:517–536.

Garee JP, Oesterreich S. 2010. SAFB1's multiple functions in biological control-lots still to be done! J Cell Biochem 109:312–319.

Graham JD, Hanson AR, Croft AJ, Fox AH, Clarke CL. 2008. Nuclear matrix binding is critical for progesterone receptor movement into nuclear foci. FASEB J 23:546–556.

Hager GL, Nagaich AK, Johnson TA, Walker DA, John S. 2004. Dynamics of nuclear receptor movement and transcription. Biochim Biophys Acta Gene Structure and Expression 1677:46–51.

Hager GL, Elbi C, Johnson TA, Voss T, Nagaich AK, Schiltz RL, Qiu Y, John S. 2006. Chromatin dynamics and the evolution of alternate promoter states. Chromosome Res 14:107–116.

Hager GL, Lim CS, Elbi C, Baumann CT. 2000. Trafficking of nuclear receptors in living cells. J Steroid Biochem Mol Biol 74:249–254.

Hager GL, McNally JG, Misteli T. 2009. Transcription dynamics. Mol Cell 35:741–753.

Hammerich-Hille S, Bardout VJ, Hilsenbeck SG, Osborne CK, Oesterreich S. 2009. Low SAFB levels are associated with worse outcome in breast cancer patients. Breast Cancer Res Treat 121:503–509.

Hart LL, Davie JR. 2002. The estrogen receptor: More than the average transcription factor. Biochem Cell Biol 80:335–341.

Htun H, Holth LT, Walker D, Davie JR, Hager GL. 1999. Direct visualization of the human estrogen receptor alpha reveals a role for ligand in the nuclear distribution of the receptor. Mol Biol Cell 10:471–486.

Inoue A, Yoshida N, Omoto Y, Oguchi S, Yamori T, Kiyama R, Hayashi S. 2002. Development of cDNA microarray for expression profiling of estrogen-responsive genes. J Mol Endocrinol 29:175–192.

Kawata M, Matsuda K, Nishi M, Ogawa H, Ochiai I. 2001. Intracellular dynamics of steroid hormone receptor. Neurosci Res 40:197–203.

Kino T, Liou S-H, Charmandari E, Chrousos GP. 2006. Glucocorticoid receptor mutants demonstrate increased motility inside the nucleus of living cells: Time of fluorescence recovery after photobleaching (FRAP) is an integrated measure of receptor function. Mol Med 10:80–88.

Kitagawa T, Matsuda KI, Inui S, Takenaka H, Katoh N, Itami S, Kishimoto S, Kawata M. 2009. Keratinocyte growth inhibition through the modification of Wnt signaling by androgen in balding dermal papilla cells. J Clin Endocr Metab 94:1288–1294.

Maruvada P. 2002. Dynamic shuttling and intranuclear mobility of nuclear hormone receptors. J Biological Chem 278:12425–12432.

Maruyama K, Endoh H, Sasaki-Iwaoka H, Kanou H, Shimaya E, Hashimoto S, Kato S, Kawashima H. 1998. A novel isoform of rat estrogen receptor beta with 18 amino acid insertion in the ligand binding domain as a putative dominant negative regular of estrogen action. Biochem Biophys Res Commun 246:142–147.

Matsuda K, Nishi M, Takaya H, Kaku N, Kawata M. 2008. Intranuclear mobility of estrogen receptor α and progesterone receptors in association with nuclear matrix dynamics. J Cell Biochem 103:136–148.

Matsuda K, Ochiai I, Nishi M, Kawata M. 2002. Colocalization and ligand-dependent discrete distribution of the estrogen receptor (ER)alpha and ERbeta. Mol Endocrinol 16:2215–2230.

McKenna NJ, Lanz RB, O'Malley BW. 1999. Nuclear receptor coregulators: Cellular and molecular biology. Endocr Rev 20:321–344.

McNally JG, Muller WG, Walker D, Wolford R, Hager GL. 2000. The glucocorticoid receptor: Rapid exchange with regulatory sites in living cells. Science 287:1262–1265.

Miller BJ, Wang D, Krahe R, Wright FA. 2003. Pooled analysis of loss of heterozygosity in breast cancer: A genome scan provides comparative evidence for multiple tumor suppressors and identifies novel candidate regions. Am J Hum Genet 73:748–767.

Moggs JG, Orphanides G. 2001. Estrogen receptors: Orchestrators of pleiotropic cellular responses. EMBO Rep 2:775–781.

Ochiai I, Matsuda K, Nishi M, Ozawa H, Kawata M. 2003. Imaging analysis of subcellular correlation of androgen receptor and estrogen receptor in single living cells using green fluorescent protein color variants. Mol Endocrinol 18:26–42.

Oesterreich S. 2003. Scaffold attachment factors SAFB1 and SAFB2: Innocent bystanders or critical players in breast tumorigenesis? J Cell Biochem 90:653–661.

Oesterreich S, Allredl DC, Mohsin SK, Zhang Q, Wong H, Lee AV, Osborne CK, O'Connell P. 2001. High rates of loss of heterozygosity on chromosome 19p13 in human breast cancer. Br J Cancer 84:493–498.

Osborne CK, Schiff R, Fuqua SA, Shou J. 2001. Estrogen receptor: Current understanding of its activation and modulation. Clin Cancer Res 7:4338s–4342s ; discussion 4411s-4412s.

Rayasam GV, Elbi C, Walker DA, Wolford R, Fletcher TM, Edwards DP, Hager GL. 2005. Ligand-specific dynamics of the progesterone receptor in living cells and during chromatin remodeling in vitro. Mol Cell Biol 25: 2406–2418.

Schaaf MJ, Cidlowski JA. 2003. Molecular determinants of glucocorticoid receptor mobility in living cells: The importance of ligand affinity. Mol Cell Biol 23:1922–1934.

Sergeant KA, Bourgeois CF, Dalgliesh C, Venables JP, Stevenin J, Elliott DJ. 2007. Alternative RNA splicing complexes containing the scaffold attachment factor SAFB2. J Cell Sci 120:309–319.

Stenoien DL, Mancini MG, Patel K, Allegretto EA, Smith CL, Mancini MA. 2000. Subnuclear trafficking of estrogen receptor-alpha and steroid receptor coactivator-1. Mol Endocrinol 14:518–534.

Stenoien DL, Nye AC, Mancini MG, Patel K, Dutertre M, O'Malley BW, Smith CL, Belmont AS, Mancini MA. 2001a. Ligand-mediated assembly and real-time cellular dynamics of estrogen receptor alpha-coactivator complexes in living cells. Mol Cell Biol 21:4404–4412.

Stenoien DL, Patel K, Mancini MG, Dutertre M, Smith CL, O'Malley BW, Mancini MA. 2001b. FRAP reveals that mobility of oestrogen receptor-alpha is ligand- and proteasome-dependent. Nat Cell Biol 3:15–23.

Townson SM, Dobrzycka KM, Lee AV, Air M, Deng W, Kang K, Jiang S, Kioka N, Michaelis K, Oesterreich S. 2003. SAFB2, a new scaffold attachment factor homolog and estrogen receptor corepressor. J Biol Chem 278:20059–20068.

Townson SM, Kang K, Lee AV, Oesterreich S. 2004. Structure-function analysis of the estrogen receptor corepressor scaffold attachment factor-

B1: Identification of a potent transcriptional repression domain. J Biol Chem 279:26074–26081.

Townson SM, Sullivan T, Zhang Q, Clark GM, Osborne CK, Lee AV, Oesterreich S. 2000. HET/SAF-B overexpression causes growth arrest and multinuclearity and is associated with aneuploidy in human breast cancer. Clin Cancer Res 6:3788–3796.

Tsutsui KM, Sano K, Tsutsui K. 2005. Dynamic view of the nuclear matrix. Acta Med Okayama 59:113–120.

van Steensel B, Jenster G, Damm K, Brinkmann AO, van Driel R. 1995. Domains of the human androgen receptor and glucocorticoid receptor involved in binding to the nuclear matrix. J Cell Biochem 57:465–478.

Verheijen R, van Venrooij W, Ramaekers F. 1988. The nuclear matrix: Structure and composition. J Cell Sci 90(Pt 1):11–36.

Wu Y, Kawate H, Ohnaka K, Nawata H, Takayanagi R. 2006. Nuclear compartmentalization of N-CoR and its interactions with steroid receptors. Mol Cell Biol 26:6633–6655.

Zhao Y-y, Guo L, Zhao X-j, Liu H, Lei T, Ma D-j, Gao X-y. 2009. Transcriptional activation of insulin-like growth factor binding protein 6 by 17β-estradiol in SaOS-2 cells. Exp Mol Med 41:478–486.